Bulletin of the Geological Society of Malaysia, Volume 71, May 2021, pp. 215 - 226
DOI: https://doi.org/10.7186/bgsm71202117

Comparison of isotope and hydrochemical characteristics of springs in Sembalun – Rinjani Area, East Lombok, West Nusa Tenggara, Indonesia before and after the earthquake events in 2018

Satrio Satrio[1,*], Rasi Prasetio[1], B. Yoseph C.S.S. Syah Alam[1], M. Sapari D. Hadian[2], Hendarmawan Hendarmawan[2]

[1] Center for Isotopes and Radiation Application, Jakarta, Indonesia
[2] Faculty of Geological Engineering, Padjajaran University, Bandung, Indonesia
* Corresponding author email address: satrio@batan.go.id

Abstract: The current 2019 isotope and hydrochemical study of hot and cold springs in Sembalun - Rinjani area is a re-assessment of previous similar study in 2012. The aim of this study is to assess the isotope and hydrochemical characteristics of springs due to the earthquake events in 2018. After the earthquake events in 2018, the stable isotopes $\delta^{18}O$ and $\delta^{2}H$ composition of Sebau hot spring and most of cold springs is shifted into more depleted values which may indicate water-rock interaction or interaction with cold waters which has more depleted $\delta^{18}O$ and $\delta^{2}H$ values. Also, Sebau hot spring is still plotted at mixing line of meteoric and andesitic water, but still dominant meteoric water. The hydrochemical data of all cold springs and Orok river show the enrichment of Na, probably from silicates weathering or the cation exhchange. While hydrochemical composition of Sebau hot spring is significantly decreased, except SO_4, probably due to dilution with cold waters before the thermal water reach the surface. The Piper diagram showed that cold springs and Orok river are Ca-Mg-HCO_3 type before and after the earthquake events. While Sebau hot spring is shifted from Ca-Cl type into mixed Ca-Mg-Cl type after the earthquake events. The temperature of Sebau hot spring slightly decreased from 35.5 °C to 34.8 °C after the earthquake events, while Na/K geothermometer calculation also indicate decreasing of sub-surface temperature, i.e. from 146–165 °C to 130–150 °C.

Keywords: Lombok earthquake 2018, Sembalun – Rinjani, springs, stable isotope, hydrochemical, geothermometer

INTRODUCTION

Sembalun – Rinjani area is located at the eastern flank of Mount Rinjani between 800–1000 m above sea level (m a.s.l.), East Lombok regency, extending about 217.8 km^2. Several cold springs are discharged at the Sembalun valley and being utilized by local inhabitants. While on the slope of Mount Rinjani, several hot springs emerged, namely Aik Kalak, Orok, Sebau and Goa Susu, which indicates geothermal potential in the area. Based on previous isotopes and hydrochemical study, the geothermal fluid has mature water characteristics and the sub-surface temperature is about 165 ^{o}C (Hadi *et al*., 2007), which can be further developed as medium-enthalpy resource (KESDM, 2017). A series of earthquake events, i.e. on July 28th 2018 (6.9 Richter Scale) and August 5th 2018 (7.0 Richter scale) struck the Lombok island, damaging not only the urban areas but also in mountainous area such as Sembalun – Rinjani, in form of landslides (Tim Pusat Studi Gempa, 2018). These earthquake events raised question whether it affected the hydrogeology system of Sembalun – Rinjani area or not.

Based on this consideration, it is necessary to re-assess the hydrochemical and isotopes characteristics of several springs in Sembalun – Rinjani area to infer the effect of earthquake events on hydrochemical characteristics. The approach of this study is using stable isotope ($\delta^{18}O$, $\delta^{2}H$) and hydrochemical method to infer the origin of cold and hot springs, water-rock interaction (Mwangi, 2013; Chenaker *et al*., 2017) and sub-surface temperature (Hou *et al*., 2018). Study on groundwater characteristics related to earthquake events has been carried out by several researchers before, such as Malakootian & Nouri (2010), Hosono *et al*. (2018) and Cox *et al*. (2015).

STUDY AREA

The study area is stretched within three sub-districts, i.e. Suela, Aikmal and Sembalun sub-districts, East Lombok Regency, West Nusa Tenggara Province – Indonesia. Geographically, the study area is located between 116º30'00" – 116º35'00" east longitude and 8º20'30" – 8º30' 00" south latitude, with area about 10 x 19 km^2 (Hadi *et al*., 2007).

GEOLOGICAL SETTING

Sembalun area is a valley that formed from old volcano caldera known as Sembalun Caldera (Figure 2), with area about 1 km^2 and relatively plain morphology at the bottom with elevation about 1000 m a.s.l. There are several cold springs at the valley of Sembalun, also the Orok river stream.

0126-6187; 2637-109X / © 2021 Geological Society of Malaysia. All rights reserved.

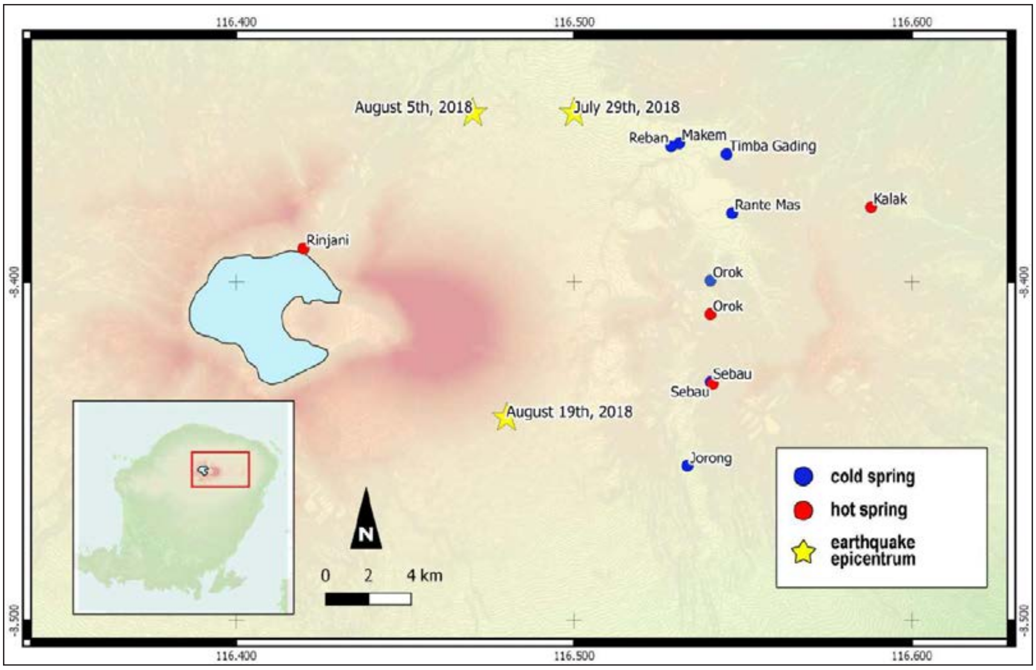
116.400
116.500
116.600
-8.400
-8.500
August 5th, 2018
July 29th, 2018
Reban
Makem
Timba Gading
Rante Mas
Kalak
Rinjani
Orok
Orok
Sebau
Sebau
August 19th, 2018
Jorong
N
0 2 4 km
cold spring
hot spring
earthquake epicentrum

Figure 1: Sampling location in Sembalun – Rinjani area, West Nusa Tenggara, Indonesia.

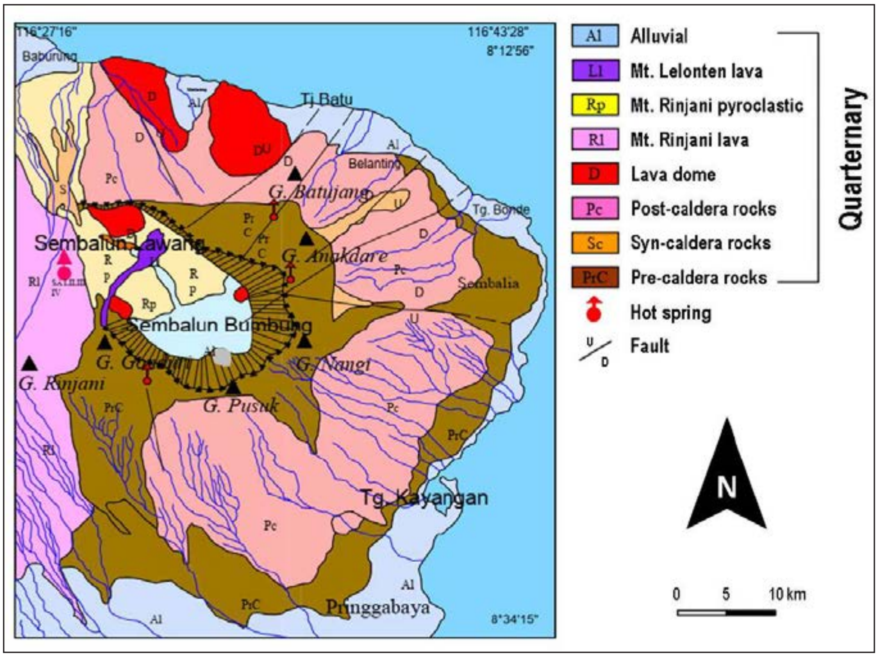
116°27'16"
116°43'28"
8°12'56"
8°34'15"
Baburung
Tj.Batu
Belanting
Tg. Bonde
G. Batujang
G. Anakdare
Sembalun Lawang
Sembalun Bumbung
Sembalia
G. Rinjani
G. Gomong
G. Nangi
G. Pusuk
Tg. Kayangan
Pringgabaya
Al Alluvial
Ll Mt. Lelonten lava
Rp Mt. Rinjani pyroclastic
Rl Mt. Rinjani lava
D Lava dome
Pc Post-caldera rocks
Sc Syn-caldera rocks
PrC Pre-caldera rocks
Quaternary
Hot spring
U/D Fault
N
0 5 10 km

Figure 2: Geological map of Sembalun – Rinjani, East Lombok, West Nusa Tenggara, Indonesia (source: Sundhoro *et al*., 2000).

While in the southern area of Sembalun, there is Sebau hot spring that indicates the geothermal activity in the area. The geothermal system in Sembalun area is related to the formation of Quaternary Sembalun old volcanic (Nasution *et al*., 2010) dominated by andesitic rocks, and there are some exposed dacitic-ryolitic rocks at the bottom of Sembalun caldera. Under the Quaternary volcanic rocks are Pliocene-Plistocene volcanic rocks composed of volcanic breccias, tuff sandstones, lava, tuffstones, lava and calcareous breccia. The rock is covered by calcarenite limestone of the Late Miocene formation. Geological structures that developed were in the form of sliding faults and normal faults trending northwest-southeast (Bakti *et al*., 2012).

The primary minerals present in the Quaternary volcanic are mainly feldspar-plagioclase ($NaAlSi_3O_8$–$CaAl_2Si_2O_8$), orthopyroxene [$Mg(Fe)_2Si_2O_6$], clinopyroxene (such as pigeonite: $Mg,Fe^{2+},Ca)_2Si_2O_6$ and calcic pyroxene (augite): [$(Ca,Mg,Fe^{2+},Fe^{3+},Al)_2(Si,Al)_2O_6$] and volcanic glass (Sundhoro *et al*., 2000). Volcanic glass is the amorphous (uncrystallized) product of rapidly cooling magma with high silica (SiO_2) content (Reka *et al*., 2019). Meanwhile, some thermal features including hot springs, and altered rocks in Sembalun geothermal area occurred in the NE–SW, W–E, NW–SE trending faults, and at the foot of Mt. Rinjani. The dominant regional strikes are heading in NW–SE and NE–SW directions (Febriani *et al.*, 2017).

Sebau hot spring is located in the south-eastern part of the National Park Mt. Rinjani, emerging as an indicator of the potential of geothermal energy in the study area and appearing as a result of the structure that leads to this location from geothermal sources around the area of the Old Caldera Sembalun. Thermal features of Orok and Sebau are controlled by Orok fault, Tanakiabang fault and the caldera wall of Sembalun (Hadi *et al.*, 2007). PIMA analysis of hydrothermal altered rocks showed the existence of clay minerals such as montmorillonite $[(Na,Ca)0.33(Al,Mg)_2(Si_4O_{10})(OH)_2.nH_2O]$, halloysite $[(Al_2Si_2O_5(OH)_4.2H_2O)]$ and paragonite $[NaAl_2(OH)_2|AlSi_3O_{10}]$ (Hadi *et al.*, 2007). The presence of these minerals will certainly affect the hydrochemical water, especially the presence of Ca^{2+} and Na^+ cations as part of the results of the alteration process.

METHOD

The hot springs, cold spring and river water samples were taken from study area (Figure 1), where field measurements i.e. temperature, pH and electric conductivity were done.

Water sampling

Groundwater sampling from a number of springs has been carried out in May 2012 and November 2019. Water samples were taken at the discharge point of the springs. Samples for cation analysis were acidified with HNO_3 (Armannsonsson & Olafsson, 2007), while samples for anion analysis were not acidified (Marini, 2000). Samples for isotopes analysis (^{18}O and ^2H) were collected in 30 mL air-tight bottle with no air bubbles to minimize isotope fractionation (Meng *et al.*, 2015; Wijatna *et al.*, 2017).

Analysis of stable isotopes of ^2H and ^{18}O

Analysis of stable isotopes of ^2H and ^{18}O of water sample was carried out in the hydrology and geothermal lab, Center for Isotope and Radiation Application, National Nuclear Energy Agency – Jakarta. Analysis of stable isotopes were done by laser spectroscopic method, i.e. using LGR (Los Gatos Research) DLT-100 Liquid Water Isotope Analyzer. Composition of isotopes is expressed as relative ratio (d) against Standard Mean Ocean Water (SMOW) following Hahed (2014):

$$\delta=(R_{Sample} - R_{SMOW}) / R_{SMOW} \times 1000‰$$

where,

R_{sample} = the isotope ratio (δ^2H or $\delta^{18}O$) of the sample, in ‰

R_{SMOW} = the isotope ratio (δ^2H or $\delta^{18}O$) of the SMOW.

Analysis of hydrochemical

Analysis of hydrochemical (major ions) was done using two methods, i.e. acid-base titration for HCO_3^- using HCl as titrant, while Ion Chromatography Metrohm 830IC was used to analyze Cl^-, SO_4^{2-} and Na^+, K^+, Ca^{2+}, Mg^{2+}.

RESULTS AND DISCUSSION

Physical and chemical characteristics

Table 1 and Table 2 show the location and physical parameters of hot springs, cold springs and river water in Sembalun – Rinjani area, for both samplings in 2012 (before the 2018 earthquake events) and in 2019 (after the 2018 earthquake events).

Hot/warm springs

Sebau warm spring is located at the southern side of Sembalun, at 1345 masl. Compared with previous study in 2012 (Satrio *et al.*, 2020), the current study in 2019 shows that the water is still blackish with temperature decreasing 0.6 °C from 35.4 °C to 34.8 °C and TDS is also decreasing from 1334 mg/L to 1064 mg/L, while the pH is relatively the same, i.e. 7.20. While Rinjani hot spring, which is located in the northeast of Sagara Anak lake at 2003 masl, has temperature of 45.0 °C (ambient temperature 18.0 °C), relatively neutral pH of 6.34 and highest TDS i.e. 4327 mg/L. Kalak hot spring which is located at the eastern side of mount Rinjani at 1050 masl, has temperature of 43.8 °C (ambient temperature 23.9 °C), neutral pH 7.06 and TDS 1462 mg/L. However, Rinjani hot spring and Kalak hot spring samples could not be collected due to a massive landslide along the route after the 2018 earthquake events.

Orok warm spring and Orok River

In 2012, the Orok warm spring was located at the Orok riverbanks at 1291 m a.s.l. with blackish color and temperature of 23.5 °C (ambient temperature 21.3 °C). The pH of the water was 7.33 and TDS of 733 mg/L. In 2019 (after the 2018 earthquake events), the Orok warm spring is no longer found. While the Orok River has temperature between 19–20 °C, with TDS content decreasing from 230 mg/L to 167 mg/L and pH also decreasing from 7.76 to 6.50.

Cold springs

Compared to the previous study, the temperature of cold springs are relatively constant between 18.3 °C to 22.2 °C in 2012 and 18.8 °C to 22.4 °C in 2019, while the pH from 6.20–8.01 to 6.50–7.13, and TDS from 172–382 mg/L to 144–282 mg/L.

Isotope characteristics

The result of isotopes analysis can be seen in Table 3, while the graph relation between $\delta^{18}O$ and δ^2H can be seen in Figure 3 and this result is utilized to infer the characteristics and origin of water samples (Diaz & Ceron, 2018).

Table 1: Location and physical parameters of hot springs, cold springs and river in Sembalun – Rinjani area, sampling 2012 (before the 2018 earthquake events).

No.	Location	Coordinate	Elevation (m asl)	T ambient (°C)	T sample (°C)	pH	TDS (mg/L)
1	Sebau cold spring	S: 9068190.01 E: 449402.07	1331	26.5	18.3	7.90	172
2	Sebau hot spring	S: 9068128.66 E: 449466.36	1345	26.5	35.4	7.35	1334
3	Rante Mas cold spring	S: 9073708.56 E: 450105.73	1205	22.5	20.9	7.01	138
4	Jorong cold spring	S: 9065445.52 E: 448653.11	1282	21.4	20.4	7.70	181
5	Timba Gading cold spring	S: 9075638.18 E: 449926.74	1162	21.0	20.5	6.20	382
6	Makem cold spring	S: 9075992.30 E: 448380.59	1152	22.5	22.2	6.65	267
7	Reban cold spring	S: 9075893.71 E: 448111.56	1297	22.5	21.2	8.01	237
8	Orok River	S: 9071509.79 E: 449395.12	1291	21.3	20.1	7.76	230
9	Orok warm spring	S: 9071509.79 E: 449395.12	1291	21.3	23.5	7.33	733
10	Rinjani hot spring	S: 9072534.25 E: 436143.50	2003	18.0	45.0	6.34	4327
11	Kalak hot spring	S: 9073907.93 E: 454634.22	1050	23.9	43.8	7.06	1462

Table 2: Location and physical parameters of hot springs, cold springs and river in Sembalun – Rinjani area, sampling 2019 (after the 2018 earthquake events).

No.	Location	Coordinate	Elevation (masl)	T ambient (°C)	T sample (°C)	pH	TDS (mg/L)
1	Sebau cold spring	S: 9068190.01 E: 449402.07	1331	25.2	18.8	7.00	144
2	Sebau hot spring	S: 9068128.66 E: 449466.36	1345	25.5	34.8	7.20	1064
3	Rante Mas cold spring	S: 9073708.56 E: 450105.73	1205	24.3	20.1	7.00	151
4	Jorong cold spring	S: 9065445.52 E: 448653.11	1282	25.2	22.4	6.80	174
5	Timba Gading cold spring	S: 9075638.18 E: 449926.74	1162	24.5	21.5	7.13	282
6	Makem cold spring	S: 9075992.30 E: 448380.59	1152	23.8	20.2	6.65	272
7	Reban cold spring	S: 9075893.71 E: 448111.56	1297	23.7	19.0	6.50	199
8	Orok River	S: 9071509.79 E: 449395.12	1291	23.8	19.2	6.50	167
9*	Orok warm spring	S: 9071509.79 E: 449395.12	-	-	-	-	-
10**	Rinjani hot spring	S: 9072534.25 E: 436143.50	-	-	-	-	-
11**	Kalak hot spring	S: 9073907.93 E: 454634.22	-	-	-	-	-

*the warm spring could not be located after the 2018 earthquake events.
**there was no access to these springs due to massive landslide after the 2018 earthquake events.

Table 3: The result of isotop $\delta^{18}O$ dan δ^2H analysis of springs and river water in the study area.

No.	Location	2012		2019	
		$\delta^{18}O$ (‰)	δ^2H (‰)	$\delta^{18}O$ (‰)	δ^2H (‰)
1	Sebau hot spring (sampling-1)	-5.50	-41.4	-5.78	-41.6
	Sebau hot spring (sampling-2)	-5.41	-42.7	-	-
2	Sebau cold spring	-6.75	-44.3	-6.76	-45.3
3	Rante Mas cold spring	-6.95	-48.8	-6.99	-49.2
4	Jorong cold spring	-6.73	-50.0	-7.51	-50.7
5	Timba Gading cold spring	-6.78	-45.5	-6.83	-44.7
6	Makem cold spring	-7.04	-49.9	-6.30	-50.5
7	Reban cold spring	-7.09	-51.3	-7.97	-51.1
8	Orok River	-6.77	-47.0	-6.33	-46.1
9	Orok warm spring	-5.59	-46.3	-	-
10	Rinjani hot spring	−2.09	−34.1	-	-
11	Kalak hot spring	-6.62	-49.3	-	-

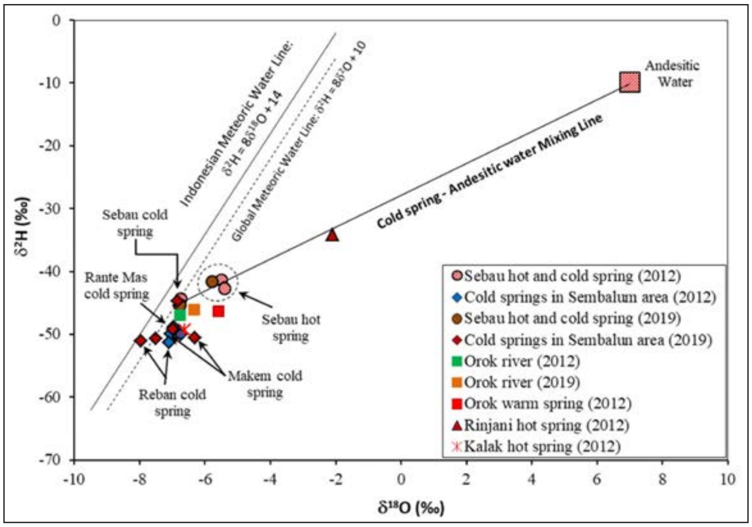

Figure 3: Graph of δ^2H vs $\delta^{18}O$ of springs and river water in the study area.

Cold springs and Orok River

The results of current stable isotopes analysis show that most of the cold springs isotope composition are shifted, i.e. varied between –0.88‰ to +0.44‰ for $\delta^{18}O$ and –1.0‰ to +0.9‰ for δ^2H, except Rante Mas cold spring that is relatively constant. The highest δ^2H shifting was found at Timba Gading cold spring, i.e. 0.8‰ which is insignificant. While $\delta^{18}O$ of Reban cold spring is shifted into more depleted value while relatively maintaining its δ^2H composition. This might indicate water-rock interaction with high oxygen content minerals such as silicates or calcite (Pang *et al.*, 2017). On the contrary, $\delta^{18}O$ of Makem cold spring is shifted into more enriched value while relatively maintaining its δ^2H value, which might suggest oxygen shifting due to interaction with silicate minerals such as feldspar-plagiocase with the reaction as shown below. As explained in the geological map, feldspar-plagiocase is one of the primary rocks of Quaternary age in the study area.

$$H_2O \leftrightarrow (NaAlSi_3O_8 - CaAl_2Si_2O_8)$$

While the $\delta^{18}O$ and δ^2H values of Orok River were shifting into more enriched values, indicating evaporation due to elongated drought season and high annual temperature (IAEA, 2015) during the 2019 event.

Hot and warm springs

The $\delta^{18}O$ and δ^2H composition of Sebau hot spring (Figure 3) shows more depleted values in 2019, –0.37‰ to -0.28‰ and +1.1 ‰ for $\delta^{18}O$ and δ^2H, respectively, i.e. from -5.50‰ and -41.4‰ (1st sampling, 2012), -5.41‰ and -42.7‰ (2nd sampling, 2012) into -5.78‰ and -41.6‰ (2019) for $\delta^{18}O$ and δ^2H, respectively. There are two possibilities for this phenomenon: (1) interaction with oxygen-hydrogen bearing minerals through mineral dissolution process, (2) interaction/mixing with cold waters which has more depleted $\delta^{18}O$ and $\delta^{2}H$ values (Wang *et al*., 2017). As explained in the geological map, the hydrothermal minerals found in the study area are montmorillonite, halloysite and paragonite, thus the ^{18}O and ^{2}H isotopes may interact with these minerals. The interaction between minerals or cold waters may cause the decrease of Sebau hot spring temperature (Long *et al*., 2019), from 35.4 °C to 34.8 °C, decreasing 0.6 °C. However, the isotope composition of Sebau hot spring still maintains the same characteristics as from the earlier study, i.e. plotted at mixing line between meteoric water and andesitic water, with dominant meteoric component (Figure 3).

The Rinjani hot spring has the most enriched isotope composition compared to other springs, which may indicate its proximity to heat source. Similar with Sebau hot spring, the Rinjani hot spring is also plotted at mixing line between meteoric water and andesitic water. While the isotope composition of Kalak hot spring is more depleted compared to other hot springs. The difference of the isotope composition probably is due to the difference in the flow paths of fluids circulation (IAEA, 1993). The isotope composition of Orok warm spring is more enriched than isotope composition of Orok river, and showed oxygen shift (Figure 3), indicating water interaction with oxygen from rock minerals (Roulleau *et al*., 2016; Abuharara, 2017). It seems that the high contribution of cold waters caused the temperature of Orok warm spring to be not high. However, in the current study, Rinjani, Kalak and Orok warm springs samples could be taken due to blocked access and landslide materials covering the springs.

Hydrochemical characteristic

Table 4 and Table 5 show the chemical analysis result of cold springs, hot springs and river taken from Sembalun – Rinjani area before and after the 2018 earthquake events. The ionic balance of the chemical analysis was below 5%, indicating good performance of analysis.

In general, Ca^{2+} and Na^{+} are the dominant cation in the water samples, while HCO_3^- and Cl^- are the dominant anion species. As seen in Figure 4, the hydrochemical composition of HCO_3^- were relatively the same, i.e. 20.7% in 2012 and 20.6% in 2019. The composition of Na^+, K^+ and Cl^- are increased, i.e. Na^+ from 12.4% to 18%, K^+ from 1.2% to 1.4% and Cl^- from 24.5% to 27.3%. While Ca^{2+} and Mg^{2+} are relatively decreased from 26.5% and 11.5% to 24.0% and 6.1%, respectively.

Cold springs and Orok River

Based on Piper diagram (Figure 5), in 2012, all cold springs and Orok River are Ca-Mg-HCO_3 type. Rante Mas and Sebau cold springs are plotted at the cation area with no dominant type, while others such as Reban, Jorong, Makem and Timba Gading cold springs are Mg type with percentage (in meq/L) from 50.2% to 58.7% of the total cation. While at anion area, all cold springs and Orok River are HCO_3 type with 72.2% to 96.6% of the total anion.

In 2019, all cold springs and Orok River are Ca-Mg-HCO_3 type, except Makem cold spring which is Ca-Na-HCO_3 type. At the cation area, Sebau cold spring does not have dominant cation, while Rante Mas cold spring is shifted from no dominant type into Ca type with 71.7% of the total cation. Orok River has Ca type, both in 2012 and 2019,

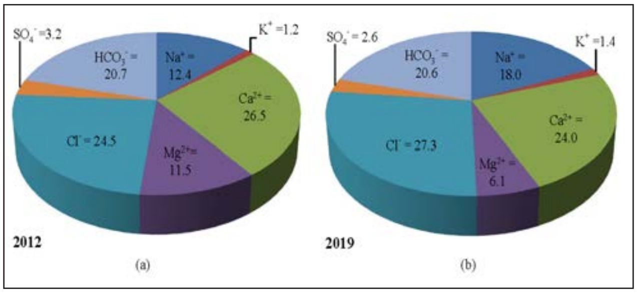

Figure 4: Hydrochemical composition (in % meq/L) in the study area: (a) 2012, and (b) 2019.

Table 4: The results of hydrochemical analysis (in mg/L) of springs and river water from sampling 2012 (before the 2018 earthquake events).

No.	Location	Na^+	K^+	Ca^{2+}	Mg^{2+}	Cl^-	SO_4^{2-}	HCO_3^-
1	Sebau cold spring	3.27	2.61	15.87	8.23	1.11	15.80	90.44
2	Sebau hot spring	170.91	6.48	291.88	11.21	647.10	15.29	146.50
3	Rante Mas cold spring	3.24	2.31	10.74	5.73	1.99	3.98	64.82
4	Jorong cold spring	4.39	3.26	10.96	9.95	2.07	0.00	100.88
5	Timba Gading cold spring	17.36	7.90	25.05	27.63	8.59	23.70	212.26
6	Makem cold spring	10.98	8.19	14.83	14.76	3.34	17.75	142.82
7	Reban cold spring	6.27	3.83	12.38	15.19	1.54	32.10	112.82
8	Orok River	4.12	2.93	27.13	13.39	5.28	9.36	105.38
9	Orok warm spring	72.27	3.24	45.16	43.29	89.23	101.05	310.00
10	Rinjani hot spring	357.95	49.67	388.66	362.91	470.89	2254.19	316.88
11	Kalak hot spring	164.42	3.45	216.02	13.67	109.06	751.92	141.38

Table 5: The results of hydrochemical analysis (in mg/L) of springs and river from sampling 2019 (after the 2018 earthquake events).

No.	Location	Na^+	K^+	Ca^{2+}	Mg^{2+}	Cl^-	SO_4^{2-}	HCO_3^-
1	Sebau cold spring	9.71	2.34	12.8	5.53	7.03	8.03	68.12
2	Sebau hot spring	164.71	4.80	174.71	3.63	572.35	16.55	91.89
3	Rante Mas cold spring	8.02	2.32	21.30	0.85	8.69	4.49	69.40
4	Jorong cold spring	10.06	3.92	17.88	4.59	7.15	4.78	83.92
5	Timba Gading cold spring	19.86	9.84	31.17	11.99	11.69	13.19	166.04
6	Makem cold spring	38.75	7.83	16.80	9.53	16.46	13.03	149.99
7	Reban cold spring	12.21	2.50	16.40	4.17	7.63	10.55	90.69
8	Orok River	10.19	3.44	25.50	7.97	8.58	12.86	109.11

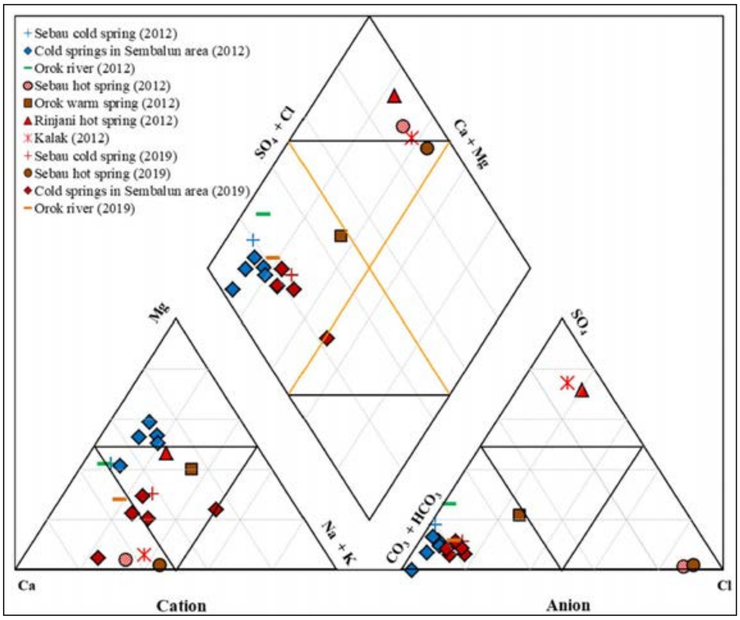

Figure 5: Piper diagram of springs in the study area.

but it is shifted from 51.16% to 53.5% of the total cation. Reban and Timba Gading cold springs are shifted from Mg type into no dominant type, while Jorong and Makem cold springs are shifted from Mg type into Ca type (52%) and Na+K type (50.8%), respectively. At the anion area, all cold springs are still the same type, i.e. HCO_3 type.

Hot and warm springs

In 2019, the chemical content of Sebau hot spring is decreasing, possibly due to dilution by cold waters before the thermal water reach the surface (Mnjokava, 2007). Also, the indication of this dilution can be seen from the TDS value which decreased from 1334 mg/L in 2012 to 1064 mg/L in 2019. The Piper diagram (Figure 5) shows that Sebau hot spring is Ca-Cl type, but Kalak and Rinjani hot springs are Ca-SO_4 type. After the 2018 earthquake events, only Sebau hot spring that still exists, while other hot springs are not accessible. Sebau hot spring is shifted from Ca-Cl type in 2012 into mixed Ca-Mg-Cl type in 2019, indicating the contribution of carbonate minerals (dolomite, calcite) or secondary mineral of montmorillonite dissolution. The process of carbonate minerals dissolution is very possible because in the study area there is limestone of the Late Miocene Formation (Tme) which is stratigraphically below the volcanic product rock as explained through the geological data above. The geological structure in the form of a normal fault plays a role in the hydrogeochemistry of the groundwater.

At cation area, Sebau and Kalak hot springs are Ca type, with each 63.6% and 56.6% of total cation, while Rinjani hot spring and Orok warm spring are of no dominant type. Although Sebau hot spring is as consistent as Ca type before and after the earthquake events, but the ion concentration decreased about 5.85 meq/L after the 2018 earthquake events.

At the anion area, in 2012, Kalak and Rinjani hot springs are plotted at SO_4 with percentage of 74.4% and 71.8% of the total anion, respectively, indicate that the waters are dominated by gypsum ($CaSO_4.2H_2O$) dissolution. Meanwhile, Sebau hot spring is consistent at Cl corner, both in 2012 and 2019, but the Cl^- concentration decreased about 2.11 meq/L in 2019 (after the 2018 earthquake events). The presence of SO_4^{2-} and Cl^- anions indicates the result

Table 6: The water types of all samples in the study area.

No.	Location	2012 Water type	2019 Water type
1	Sebau cold spring	Ca-Mg-HCO_3	Ca-Mg-HCO_3
2	Sebau hot spring	CaCl	Mixed Ca-Mg-Cl
3	Rante Mas cold spring	Ca-Mg-HCO_3	Ca-Mg-HCO_3
4	Jorong cold spring	Ca-Mg-HCO_3	Ca-Mg-HCO_3
5	Timba Gading cold spring	Ca-Mg-HCO_3	Ca-Mg-HCO_3
6	Makem cold spring	Ca-Mg-HCO_3	Mixed Ca-Na-HCO_3
7	Reban cold spring	Ca-Mg-HCO_3	Ca-Mg-HCO_3
8	Orok River	Ca-Mg-HCO_3	Ca-Mg-HCO_3
9	Orok warm spring	Ca-Mg-HCO_3	-
10	Rinjani hot spring	Ca-SO_4	-
11	Kalak hot spring	Ca-SO_4	-

of mineral dissolution in rocks deposited in the marine environment related to the formation of limestone Ekas Formation. While, Orok warm spring is plotted at HCO_3 corner or HCO_3 type with percentage of 53.4% of total anion and tend to have mixed Ca-Mg-Cl type, that may indicate dissolution of dolomite and halite.

Table 6 shows the water types from all samples (warm spring, hot spring, cold spring and river water) in the study area, both in 2012 and 2019.

Hydrochemical control of groundwater

The main source of dissolved Na^+ and K^+ is silicate minerals weathering. As commonly known, minerals of igneous rocks such as pyroxenes, amphiboles, calcic and potassium feldspar are prone to silicate weathering. The weathering will enrich the Na^+ and K^+ concentration of groundwater. The end product of the silicate weathering can produce a variety of materials, mostly clay (Kumar & James, 2016). Silicate weathering that controlled groundwater chemical composition can be described using graph relation between (Ca^{2+}+Mg^{2+}) and total cations (Figure 6a). It is shown that all samples are plotted at 1:1 line which means that all samples show Na^+ release as a result of silicate weathering process (Toscano *et al*., 2020). Meanwhile, the increasing of Na^+ concentration of all cold spring and Orok River in 2019 or after the 2018 earthquake events can be explained by using Na^+ vs Cl^- graph (Figure 6b and 6c) (Chenini *et al*., 2015). Based on the graph, most of the samples are plotted above the equiline 1:1, i.e. Na^+/Cl^- ratio >1, which indicates addition of Na^+ from silicate weathering or a cation exchange (Zhang *et al*., 2020), while Cl^- addition to cold springs may originate from halite dissolution that increased after the 2018 earthquake events. Figure 6d, the graph of the relationship of $Ca^{2+}+Mg^{2+}$ vs $HCO_3^-+SO_4^{2-}$ shows that almost all cold springs, Orok River and Orok warm spring are along the equiline, indicating that the abundance of these ions is mainly due to the weathering of carbonates (calcite and dolomite) (Mora *et al*., 2017). For Sebau hot spring (2012 and 2019) shows those points fall above the equiline, indicating that dolomite or montmorillonite secondary minerals dissolution was the primary process determining the chemical of groundwater (Vasu *et al*., 2017). While, Kalak and Rinjani hot springs show those points fall below the equiline, indicating gypsum or anhydrite dissolution was the primary process determining the chemical of groundwater. Both minerals are indicated to be related to the limestone of the Ekas Formation which forms the base of volcanic rocks formed in the marine environment.

The hydrochemical control of groundwater can be assessed by using Gibs diagram (Gibss, 1970), which generally consists of three controlling processes, i.e. precipitation (rain fall), evaporation-crystallization and water-rock interaction (Wu *et al*., 2018). Gibbs constructed simple but effective diagram using TDS vs $Na^+/(Na^++Ca^{2+})$ and TDS vs $Cl^-/(Cl^-+HCO_3^-)$ relation to identify the influencing factors of groundwater hydrochemical (Luo *et al*., 2018). Figure 7 shows that hydrochemical process at all cold springs and Orok River are dominantly controlled by water-rock interaction mechanism. While all hot springs and Orok warm spring tend to be controlled by evaporation crystallization, which indicate dissolution of evaporite minerals such as halite and gypsum.

In 2012, the $Na^+/(Na^++Ca^{2+})$ ratios of all cold springs and Orok River are varied from 0.17 to 0.43 with average of 0.28, while $Cl^-/(Cl^-+HCO_3^-)$ ratios are varied from 0.01 to 0.05 with average of 0.03, suggesting a strong cation exchange in the groundwater system (Gao *et al*., 2019). In 2019, the average ratios of $Na^+/(Na^++Ca^{2+})$ and $Cl^-/(Cl^-+HCO_3^-)$ of all cold springs and Orok river are 0.41 and 0.09, respectively, which indicate dominant cation exchange also. However, the ratios from Sebau, Kalak and Rinjani hot springs suggest a strong anion exchange, while the ratio from Orok warm spring strongly suggest cation exchange. Also, the increasing Na^+ ion after a series of earthquakes in 2018 followed by the decreasing Mg^{2+} ion in all cold

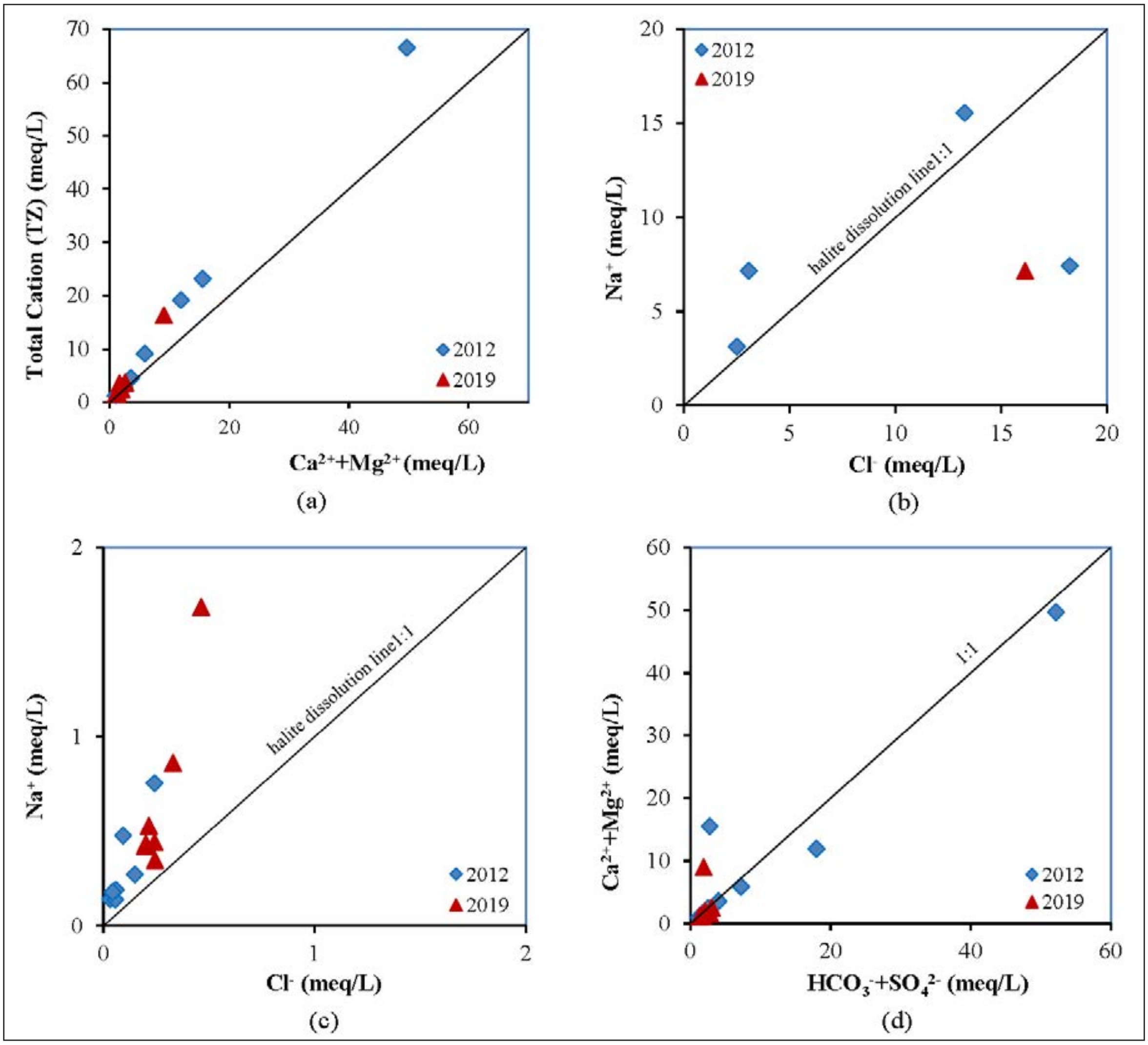

Figure 6: Graph of: (a) Total cation vs $Ca^{2+}+Mg^{2+}$, b) Na^+ vs Cl^- from hot and warm springs, (c) Na^+ vs Cl^- from cold springs and river water, (d) $Ca^{2+}+Mg^{2+}$ vs $HCO_3^-+SO_4^{2-}$.

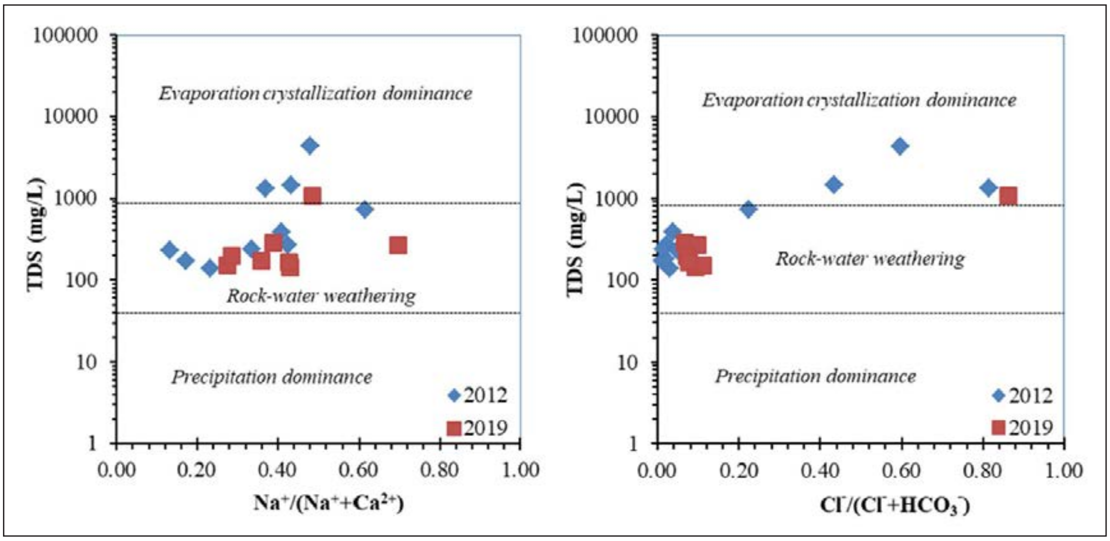

Figure 7: Gibbs diagram of springs and river water.

springs is indicated from the cation exchange process, i.e. the ionic exchange between Mg^{2+} of the groundwater with Na^+ of the silicate minerals, resulting in Na^+ concentration increases and Mg^{2+} concentration decreases in groundwater (Huang & Ma, 2019). The cation exchange process is the following reaction.

Geothermometer

The sub surface temperature calculation is based on specific chemical equilibrium reaction such as Na and K. The current study used Na/K and silica geothermometers formulated by Fornier and Giggenbach (Wishart, 2015). The result of geothermometer calculation of Sebau hot spring, both in 2012 (before the 2018 earthquake events) and 2019 (after the 2018 earthquake events) is presented in Table 7.

Based on Na/K geothermometer formulated by Fournier and Giggenbach, the sub surface temperature of Sebau hot spring decreased from 146–165 ^oC to 130–150 ^oC after the 2018 earthquake events. While quartz geothermometer calculation decreased from 94 ^oC (SiO_2=40.69 mg/L) to 85 ^oC (SiO_2=31.38 mg/L). Temperature calculated from quartz geothermometer is lower than calculated from Na/K geothermometer due to fast re-equilibrium of silica compared to Na and K, thus the temperature from quartz geothermometer is shallower sub-surface temperature (Wishart, 2013). This decrease in temperatures is possibly due to the process of dilution by cold waters as explained in the discussion above (Lajwe, 2013).

CONCLUSIONS

After the earthquake events in 2018, there has been a change in the isotopes values compared to before (2012), i.e. most of the cold springs were shifted into more depleted values. The shifting phenomenon is possibly due to the interaction with rock minerals such as carbonates (calcite, dolomite) or silicates. However, the characteristics are still the same as previous study, i.e. represents the meteoric water. While Sebau hot spring also shows interaction with rock minerals, thus the $\delta^{18}O$ and δ^2H were slightly shifting into more depleted values toward the meteoric water line, which indicates interaction/mixing with minerals or cold waters which has more depleted $\delta^{18}O$ and δ^2H values. Mineral alteration data of study area show the existence of clay minerals such as montmorillonite which interacted with water and shifted its ^{18}O and δ^2H value. The characteristics of Sebau hot spring are still the same as previous study, i.e. plotted at mixing line between meteoric water and andesitic water with dominant meteoric component.

Based on the 2019 hydrochemical data of all cold spring and Orok river, there is an increasing Na^+ and Cl^- concentration followed by decreasing Mg^{2+} concentration, which indicates addition of Na^+ from silicate weathering or the cation exhchange. Meanwhile, there is a decreasing Na^+ and Cl^- concentration in Sebau hot spring, which may indicate dilution of thermal water with cold waters before discharging in the surface. Also, the indication of this dilution can be seen from the TDS value which decreased from 1334 mg/L in 2012 to 1064 mg/L in 2019.

Based on Piper diagram, before the 2018 earthquake events, all cold springs and Orok River are Ca-Mg-HCO_3 type. In 2019 or after the 2018 earthquake events, most of cold springs and Orok River are Ca-Mg-HCO_3 type, while Makem cold spring is Ca-Na-HCO_3 type. As for Sebau hot spring, it is shifted from Ca-Cl type into mixed Ca-Mg-Cl type. Gibbs diagram shows that the hydrochemical process of all cold spring and Orok river is predominant by cation exchange process, controlled through water-rock interaction mechanism. Meanwhile, all hot springs are predominant by anionic exchange process, controlled by dissolution of evaporite mineral.

This study also shows that the temperature of Sebau hot spring decreased from 35.4 ^oC to 34.8 ^oC, while Na/K geothermometer calculation also showed a decreasing sub-surface temperature from 146–165 ^oC to 130–150 ^oC, while silica quartz geothermometer decreased from 94 ^oC to 85 ^oC.

ACKNOWLEDGEMENTS

The authors would like to thank the head of Rinjani volcano surveillance office and the staff for the assistance during the sampling campaign in Sembalun, East Lombok. The authors also deeply appreciate the assistance from Center for Isotopes and Radiation Application, Jakarta – Indonesia during the isotope and hydrochemical analysis of the samples in the laboratory. The reviewers are also thanked for their constructive comments.

Table 7: The results of Na/K and silica (SiO_2) geothermometer calculation.

	Geothermometer (^oC)		
Location	**Na/K Fournier**	**Na/K GGB**	**SiO_2 Quartz**
Sebau hot spring (2019)	130	150	85
Sebau hot spring (2012)	146	165	94
Decrease:	16	15	9

REFERENCES

Abuharara, A., 2017. Using Isotopes to Understand the Origin of Water and the Effect of Reinjection in the Los Azufers Geothermal Field in Mexico. MSc thesis, University of Waterloo.

Armannsonsson, H. & Olafsson, M., 2007. Geothermal sampling and analysis. Short Course Geotherm. Resour. 11, 1–8.

Bakti, H., Lubis, R.F., Delinom, R. & Naily, W., 2012. Identify on submarine ground water discharge (SGD) on the alluvial coast of North Lombok, West Nusa Tenggara. Lingkung dan Bencana Geol., 3, 133–149.

Chenaker, H., Houha, B. & Vales, V., 2017. Isotope studies and chemical investigations of hot springs from North-Eastern Algeria. J. Mater. Environ. Sci., 8, 4253–4263.

Chenini, I., Farhat, B. & Mammou, A. Ben, 2015. Identification of major sources controlling groundwater chemistry from a multilayered aquifer system Identification of major sources controlling groundwater chemistry from a multilayered aquifer system. Chem. Speciat. Bioavailab., 22, 183–189.

Cox, S.C., Menzies, C.D., Sutherland, R., Denys, P.H. & Chamberlain, C., 2015. Changes in hot spring temperature and hydrogeology of the Alpine Fault hanging wall, New Zealand, induced by distal South Island earthquakes. Geofluids, 15 (1-2), 216–239. https://doi.org/10.1111/gfl.12093.

Diaz, E.G. & Ceron, M.I.M., 2018. Preliminary geochemical study of thermal waters at the Puracé volcano system (South Western Colombia): an approximation for geothermal exploration. Bol. Geol., 40, 1–20.

Febriani, F., Gaffar, E., Widarto, D.S. & Grandis, H., 2017. The magnetotelluric phase tensor analysis of the Sembalun-Propok area, West Nusa Tenggara, Indonesia. J. Phys. Conf. Ser., 817, 1–8.

Gao, Z., Liu, J., Feng, J., Wang, M. & Wu, G., 2019. Hydrogeochemical Characteristics and the Suitability of Groundwater in the Alluvial-Diluvial Plain of Southwest Shandong Province, China. Water, 11, 1–19.

Gibss, R.J., 1970. Mechanisms Controlling World Water Chemistry. Science, 170(3962), 1088–1090.

Hadi, M.N., Yushantarti, A., Suhanto, E. & Sundhoro, H., 2007. Survei Panas Bumi Terpadu (Geologi, Geokimia Dan Geofisika) Daerah Sembalun, Kabupaten Lombok Timur - Ntb. In: Proceeding Pemaparan Hasil Kegiatan Lapangan Dan Non Lapangan Tahun 2007. Pusat Sumber Daya Geologi, Bandung - Indonesia, 1–14.

Hahed, Y., 2014. Stable Isotope Ratios in Meteoric Waters in El Kef Region , Northwestern Tunisia: Implications for Changes of Moisture Sources. Earth Sci. Clim. Chang., 5, 1–6. https://doi.org/10.4172/2157-7617.1000203.

Hosono, T., Hartmann, J., Louvat, P., Amann, T., Washington, K.E., West, A.J., Okamura, K. & Böttcher, M.E., 2018. Earthquake-induced structural deformations enhance long-term solute fluxes from active volcanic systems. Sci. Rep., 8, 1–12. https://doi.org/10.1038/s41598-018-32735-1.

Hou, Y., Shi, Z. & Mu, W., 2018. Fluid Geochemistry of Fault Zone Hydrothermal System in the Yidun-Litang Area, Eastern Tibetan Plateau Geothermal Belt. Geofluids, 2018(4), 1–14.

Huang, T. & Ma, B., 2019. The Origin of Major Ions of Groundwater in a loess aquifer. Water, 11(12), 1–14.

IAEA, 1993. Isotope and geochemical techniques applied to geothermal investigations. In: Proceedings of the Final Research Co-Ordination Meeting on the Application of Isotope and Geochemical Techniques to Geothermal Exploration in the Middle East, Asia, the Pacific and Africa. Dumaguete City, Philippines, 12-15 October 1993, 1–261.

KESDM, 2017. Buku Potensi Panas Bumi Indonisia Jilid 1.

Kumar, P.J.S. & James, E.J., 2016. Identification of hydrogeochemical processes in the Coimbatore district , Tamil Nadu , India. Hydrol. Sci. J., 61, 719–731.

Lajwe, G., 2013. Comparison characterization and interpretation of geothermal fluid geochemistry in sedimentary environments of Kibiro, Panyimur and Öxarfjördur. World Geotherm. Congr., 12, 19–25.

Long, X., Zhang, K., Yuan, R., Zhang, L. & Liu, Z., 2019. Hydrogeochemical and Isotopic Constraints on the Pattern of a Deep Circulation Groundwater. Energies, 12, 1–18.

Luo, W., Gao, X. & Zhang, X., 2018. Geochemical processes controlling the groundwater chemistry and fluoride contamination in the Yuncheng Basin, China — An area with complex hydrogeochemical conditions. PLoS One, 13, 1–25.

Malakootian, M. & Nouri, J., 2010. Chemical variations of ground water affected by the earthquake in bam region. Int. J. Environ. Res., 4, 443–454.

Marini, L., 2000. Geochemical techniques for the exploration and exploitation of geothermal energy. Laboratorio di Geochimica, Università degli Studi di Genova, Genova, Italia. 82 p.

Meng, Y., Liu, G. & Li, M., 2015. Tracing the sources and processes of groundwater in an alpine glacierized region in Southwest China: Evidence from environmental isotopes. Water, 7, 2673–2690. https://doi.org/10.3390/w7062673.

Mnjokava, T.T., 2007. Interpretation of Exploration Geochemical Data for Geothermal Fluids from the Geothermal Field of the Rungwe Volcanic Area, SW Tanzania, UNU-GTP Reykjavík, Iceland, Reports.

Mora, A., Mahlknecht, J., Rosales-lagarde, L. & Hernández-antonio, A., 2017. Assessment of major ions and trace elements in groundwater supplied to the Monterrey metropolitan area, Nuevo León, Mexico. Environ Monit Assess, 189, 1–15. https://doi.org/10.1007/s10661-017-6096-y.

Mwangi, S.M., 2013. Application of Geochemical Methods in Geothermal Exploration in Kenya. Procedia Earth Planet. Sci., 7, 602–606. https://doi.org/10.1016/j.proeps.2013.03.220.

Nasution, A., Takada, A., Udibowo, Widarto, D. & Hutasoit, L., 2010. Rinjani and Propok Volcanics as a Heat Sources of Geothermal Prospects from Eastern Lombok, Indonesia. J. Geoaplika, 5, 1–9.

Pang, Z., Kong, Y., Li, J. & Tian, J., 2017. An isotopic geoindicator in the hydrological cycle. In: Procedia Earth and Planetary Science. 534–537.

Reka, A.A., Pavlovski, B., Lisichkov, K., Jashari, A., Boev, B. & Boev, I., 2019. Chemical , mineralogical and structural features of native and expanded perlite from Macedonia. J. Croat. Geol. Surv. Croat. Geol. Soc., 72, 215–221. https://doi.org/10.4154/gc.2019.18.

Roulleau, E., Tardani, D., Sano, Y., Takahata, N., Vinet, N., Bravo, F., Munoz, C. & Sanzhez, J., 2016. New insight from noble gas and stable isotopes of geothermal / hydrothermal fluids at Caviahue-Copahue Volcanic Complex : Boiling steam separation and water-rock interaction at shallow depth. J. Volcanol. Geotherm. Res., 328, 70–83.

Satrio, S., Prasetio, R., Syah Alam, B.Y.C.S.S., Iskandarsyah, T.Y.W.M., Muhammadsyah, F., Hadian, M.S.D., Hendarmawan, H., 2020. Isotope and Geochemistry Characterization of Hot

Springs and Cold Springs of Sembalun – Rinjani Area, East Lombok, West Nusa Tenggara – Indonesia. Indones. J. Chem., 20, 1347–1359. https://doi.org/10.22146/ijc.50790.

Sundhoro, H., Nasution, A. & Simanjuntak, J., 2000. Sembalun Bumbung geothermal area, Lombok Island, West Nusatenggara, Indonesia: an integrated exploration. Proc. World Geotherm. Congr. 2000, Kyushu - Tohoku, Japan, 1785–1790.

Tim Pusat Studi Gempa, 2018. Kajian Rangkaian Gempa Lombok.

Toscano, C.A.R., Villanueva, R.A.C., Martinez, R.C., Bermea, O.M., Alvarez, E.H., Delgado, O.B. & Olivera, J.A.Á., 2020. Hydrogeochemical Characteristics and Assessment of Drinking Water Quality in the Urban Area of Zamora, Mexico. Water, 12, 1–26.

Vasu, D., Singh, S.K., Tywary, P., Sahu, N., Ray, S.K., Butte, P. & Duraisami, V.P., 2017. Influence of geochemical processes on hydrochemistry and irrigation suitability of groundwater in part of semi-arid Deccan Plateau, India. Appl. Water Sci., 13, 1–13. https://doi.org/10.1007/s13201-017-0528-2.

Wang, Y., Kong, Y., Pang, Z., Yang, F. & Pang, J., 2017. Stable Isotopes of Deep Groundwater in the Xiongxian Geothermal Field. Procedia Earth Planet. Sci., 17, 512–515.

Wijatna, A.B., Kayyis, M., Satrio, S. & Pujiindiyati, E.R., 2017. Study of Seawater Intrusion in Deep Aquifers of Semarang Coast Using Natural Isotopes and Hydrochemicals. Indones. J. Geosci., 4, 159–167.

Wishart, D.N., 2015. Comparison of Silica and Cation Geothermometers of Bath Hot Springs, Jamaica WI. In: World Geothermal Congress 2015, 1–13.

Wishart, D.N., 2013. Geothermometry and Shallow Circulation of a Low Enthalpy System: the Bath Geothermal Reservoir, Jamaica. In: Thirty-Eighth Workshop on Geothermal Reservoir Engineering, 1–9.

Wu, C., Wu, X., Qian, C. & Zhu, G., 2018. Hydrogeochemistry and groundwater quality assessment of high fluoride levels in the Yanchi endorheic region, northwest China. Applied Geochemistry, 98, 404–417.

Zhang, B., Zhao, D., Zhou, P., Qu, S. & Liao, F., 2020. Hydrochemical Characteristics of Groundwater and Dominant Water – Rock Interactions in the Delingha. Water, 12, 1–16. https://doi.org/10.3390/w12030836.

Manuscript received 15 June 2020
Revised manuscript received 12 August 2020
Manuscript accepted 11 September 2020